RSC Advances

PAPER

View Article Online
View Journal | View Issue

Cite this: *RSC Adv.*, 2026, **16**, 21693

Transforming plastic waste into liquid fuels: novel upgrading of polypropylene pyrolysis oil and its utilization in a diesel engine

Abhishek Kumar Yadav,†[a] Suparna Maity,†[a] Sandeep Kumar Yadav,[a] Vasudeva Madav,[b] G. N. Kumar[b] and Saikat Dutta*[a]

Received 22nd November 2025
Accepted 15th April 2026

DOI: 10.1039/d5ra09026a

rsc.li/rsc-advances

Pyrolysis of end-of-life polypropylene (EOL-PP) items into polypropylene pyrolysis oil (PPO) is a scalable, economically feasible, and environmentally acceptable waste-to-energy pathway. The poor stability (*e.g.*, storage and oxidative) and inferior physicochemical properties (*e.g.*, low flash point) of crude PPO (CPPO) mandate an inexpensive, scalable, and eco-friendly upgrading method to enable its use as engine fuel. This work reports a novel upgrading of CPPO into upgraded PPO (UPPO) by sequentially removing the excessively volatile and chemically unstable components in a two-step process. The chemical composition of the volatile fraction (b.p. <150 °C) resembled that of gasoline and the heavy naphtha fraction, which promises to diversify the applications and markets of PPO. The physicochemical properties and spectral characteristics of CPPO and UPPO were analyzed to quantify the improvements in fuel properties. UPPO showed noticeably better physicochemical properties than CPPO. The UPPO (10–25 vol%)-diesel blends were used in a diesel engine to study the engine performance and emission characteristics, which afforded comparable engine performance (*e.g.*, brake thermal efficiency) and reduced emissions (*i.e.*, NO_x, CO, and unburnt hydrocarbons) compared to unblended diesel.

1. Introduction

The applications of polypropylene (PP) have rapidly expanded over the past two decades across various industries due to its pliable properties, including chemical and moisture resistance, light weight, high impact strength, and good moldability.[1] However, end-of-life polypropylene (EOL-PP) items have created serious environmental concerns due to their slow environmental degradation and accumulation in landfill sites.[2] Indiscriminate disposal of EOL-PP leads to pollution (air, water, and soil), posing health-, fire-, and ecological hazards.[2] A scalable, economical, and eco-friendly solution for the waste management of EOL-PP is paramount from social, economic, and environmental perspectives.[3] In this regard, pyrolysis of EOL-PP into crude polypropylene pyrolysis oil (CPPO) has shown promise due to the process simplicity, scalability, and marketability of CPPO as a hydrocarbon-based liquid fuel.[4] The hydrocarbon backbone of EOL-PP can be cleaved by heat in the absence (thermal) or presence of a catalyst (catalytic) to form a mixture of liquid hydrocarbons of varying carbon chain lengths, mainly in the diesel fuel range.[5–7] A considerable portion of a barrel of petroleum is transformed into synthetic thermoplastics (*e.g.*, PP); therefore, the production of CPPO from EOL-PP is critical in a resource-constrained world helping to reclaim the resources while minimizing waste accumulation.[8,9] The pyrolysis of EOL-PP produces CPPO, combustible gases, and carbonized char, and their relative proportions depend on the feedstock and the process parameters.[10] Even though all the components obtained during the pyrolysis process can be valorized individually, CPPO is the most important fraction due to its diverse applications and huge market potential.[11,12] Significant research has been devoted to fine-tuning the pyrolysis of EOL-PP to maximize CPPO yield and improve its quality as a liquid fuel.[13] CPPO can be used as a substitute for diesel in furnaces and diesel engines.[14] However, the inconsistent quality of CPPO produced during thermal pyrolysis of EOL-PP and its degradation during storage poses a major challenge for using it directly as furnace and engine fuel. Several process parameters, including the quality of the feedstock (*i.e.*, the extent of degradation and ageing of EOL-PP and contamination from other plastics), reactor type, pyrolysis temperature, and residence time, determine the quality of CPPO. The oxygen content in EOL-PP increases over time since the PP backbone gets partially oxidized by photooxidation, leading to oxygenated compounds in the CPPO.[15] The inferior thermal, oxidative, and storage stability of CPPO primarily originates from these polar components. Moreover, the unstable compounds produced during the pyrolysis of EOL-

[a]*Department of Chemistry, National Institute of Technology Karnataka, Surathkal, Mangalore–575025, Karnataka, India. E-mail: sdutta@nitk.edu.in*

[b]*Department of Mechanical Engineering, National Institute of Technology Karnataka, Surathkal, Mangalore–575025, Karnataka, India*

† Equal contribution.

PP, such as terminal olefins, can undergo oxidation and oligomerization, forming a waxy residue during the storage and transportation of CPPO.[16,17] Therefore, attempts have been made to improve the quality of CPPO by suitable upgrading. The upgraded PPO (UPPO) can be produced using two primary strategies. The catalytic pyrolysis of EOL-PP can produce UPPO, as the catalyst promotes selective bond cleavage at lower temperatures and minimizes the formation of unstable, undesirable compounds.[18] However, the catalysts are often expensive, and recovering them from the carbonized char is very challenging.[19] Catalyst has also been used to upgrade the CPPO from thermal pyrolysis in a separate step.[20] However, this strategy often requires expensive catalysts (*e.g.*, zeolite), additional energy (*i.e.*, heat), and a catalyst recycling setup. An alternative strategy for obtaining UPPO is to upgrade CPPO downstream *via* processes like fractional distillation. However, the process is energy-intensive, low-yielding, and produces significant waste from repolymerization and carbonization reactions.[21,22] Attempts have been made to remove the acidic and oxygenated polar compounds by preferential solubility and selective adsorption over a suitable adsorbent.[23] However, the cost of solvents and adsorbents increases the operational expenditures.[24] Attempts have been made on radical-mediated catalytic deconstruction of plastics into valuable chemicals and monomers using a uranyl-based photocatalytic system. Uranyl-based photocatalytic systems involve radioactive materials, raising concerns towards process scalability and environmental and health safety during plastic upgradation at the commercial scale.[25] We envisioned that the excessively volatile fraction (b.p. <150 °C) could be distilled from CPPO under atmospheric pressure to improve the flash point. The acid-promoted degumming process can remove the relatively unstable and waxy compounds from the remaining liquid.[26] A suitable organic or mineral acid insoluble in CPPO can react with oxygenates and unstable hydrocarbons (*e.g.*, terminal olefins) and precipitate them from the CPPO.

Typically, a multi-stage treatment and purification process is involved in acid degumming of vegetable oil.[27] For example, the oil sample must be treated with aqueous acid at high temperature or under sonication. Then the oil sample must be phase-separated, pH-adjusted with a base, and dried to remove any trace water. However, such elaborate operational steps would compromise the process's scalability and increase its cost. We reasoned that the hydrocarbon-rich CPPO is radically different from triglyceride-containing vegetable oil. Therefore, the acid-promoted degumming of CPPO can be simplified by selecting an appropriate acid catalyst.

This work shows how CPPO can be upgraded into UPPO by a two-stage process. In the first step, the excessively volatile fraction (b.p. <150 °C) from CPPO was separated by fraction distillation under atmospheric pressure. The heavier fraction was then degummed with acids to easily separate unstable

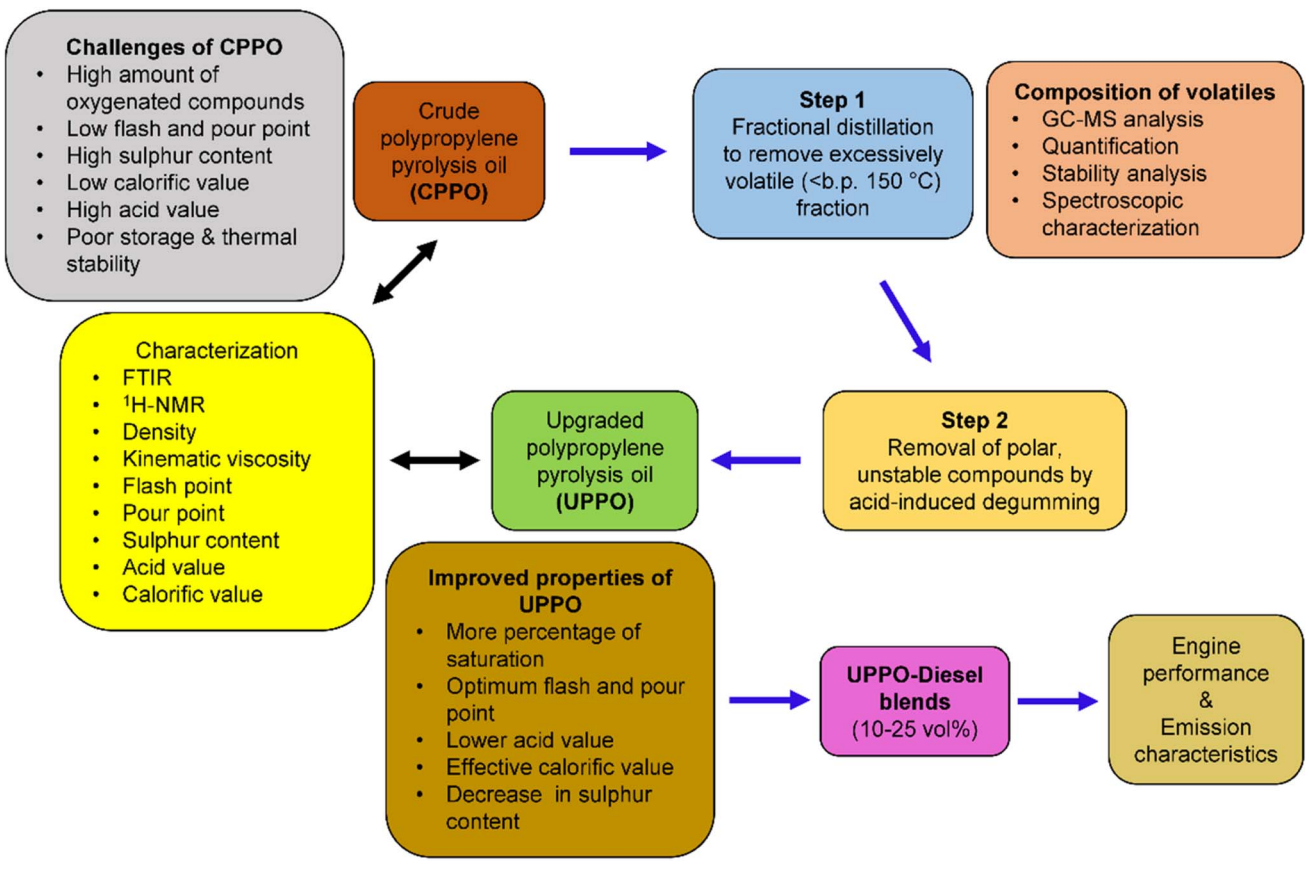

Fig. 1 Overall scheme and objectives of this work on using UPPO as an alternative liquid fuel in the diesel engine.

compounds in their oligomerized or polymerized forms. The colorless volatile fraction containing light hydrocarbons can be used as the naphtha fraction or as aviation fuel and can be conveniently integrated into the petrorefinery infrastructure. This high-value fraction can improve the economic feasibility of producing PPO from EOL-PP. The physicochemical characteristics, thermal properties, and chemical composition of CPPO and UPPO (prepared over two steps) were analyzed. The UPPO was then blended with diesel in 10–20 vol%, and the blended fuels were then used as fuels in a diesel engine (Fig. 1). The engine performance and emission characteristics of the UPPO-diesel blends were studied.

2. Experimental methodology

2.1 Materials

Crude polypropylene pyrolysis oil (CPPO) was obtained from a local PPO manufacturer. The end-of-life polypropylene chairs were used as feedstock for producing CPPO. The powdered EOL-PP was fed into a 500 kg batch reactor. The thermal pyrolysis was performed at 450 °C, which took a total of 4 h to complete. The vaporized CPPO emanating from the reactor was cooled in a water-cooled condenser and stored in HDPE drums. Diesel was purchased from a commercial outlet of the Indian Oil Corporation Limited (IOCL) in Mangalore, Karnataka. Orthophosphoric acid (85%) and polyphosphoric acid (98%) were procured from Loba Chemie Pvt. Ltd.

2.2 Instrumental analysis

The molecular composition of CPPO and UPPO was analyzed by Fourier transform infrared (FTIR), ^{1}H-NMR, and GC-MS. The FTIR spectra were recorded in a Bruker Alpha-II instrument using the attenuated total reflectance (ATR) method. A few drops of the fuel samples were diluted in dichloromethane, and a thin film was formed on the ATR counter top by evaporating a drop of the solution at room temperature. The recorded FTIR spectrum for each sample was an average of 24 scans collected at a scan rate of 4 scans per second. The selected spectral range was 600 cm^{-1} to 4000 cm^{-1} to analyze the full width of the functional group and fingerprint regions. The ^{1}H-NMR data of the fuel samples were used to study the chemical composition, H/C ratio, and iso-paraffin index of pyrolysis oil. The ^{1}H-NMR spectra were recorded on a Bruker NanoBay® NMR instrument operating at 400 MHz. Deuterated chloroform ($CDCl_3$) was chosen as the solvent for diluting the fuel samples and recording the NMR data. The gas chromatography (GC) analyses of CPPO and UPPO were performed in a LECO Pegasus BT 4D spectrometer. Given the hydrocarbon-rich composition of CPPO and UPPO, a non-polar column (Rtx-5 ms, 30 m × 0.25 mm × 0.25 μm) and a polar column (Rxi-17) were employed to help separate the compounds. High-purity helium gas was employed as the carrier gas at a constant flow rate of 1.40 mL min^{-1}. The injector temperature was fixed at 250 °C with a 100 : 1 split ratio. The oven temperature was initially set to 60 °C for 2 min, then ramped at 10 °C min^{-1} to 300 °C. LECO Chroma software was used to process the acquired chromatograms further. The compounds were characterized by mass spectrometry and matched against the library integrated into the software to determine the percentage similarity.

2.3 Upgradation of CPPO

A straightforward and scalable two-step upgradation procedure was employed to convert CPPO into UPPO. In the first step, the excessively volatile compounds in CPPO (b.p. < 150 °C), which are responsible for a very low flash point, were removed by fractional distillation under atmospheric pressure. CPPO was taken in a round-bottomed flask and placed in an electrically heated furnace. The flask was connected to a water-cooled condenser through a glass adapter. The other end of the condenser was connected to a receiver flask (a distillation setup) through another glass adapter with a vacuum joint exposed to the atmosphere. The reaction flask containing CPPO (50 mL) was heated to 150 °C until the volatile compounds distilled out and condensed in the collecting flask as a transparent liquid (Scheme 1). The heavier fraction remaining in the distillation flask was evaluated as a diesel substitute because its molecular composition matched that of diesel fuel.

In the second step of the upgrading process, the residual polypropylene pyrolysis oil (DPPO) post-distillation was treated with 3% (v/v) of orthophosphoric acid (85%) for 2 h at room temperature to remove the gum-forming and polar components (*e.g.*, oxygenates, heterocycles). The gum-forming compounds and various polar compounds (*e.g.*, oxygenates) separate. The supernatant oil was decanted and stored in sealed glass containers. It was observed that a slightly elevated temperature (50 °C) accelerated the degumming process, and the contact time was reduced significantly (<1 h). The loss during this upgrading step was found to be 5–8 vol%, depending on the quality of different batches of CPPO. The upgraded

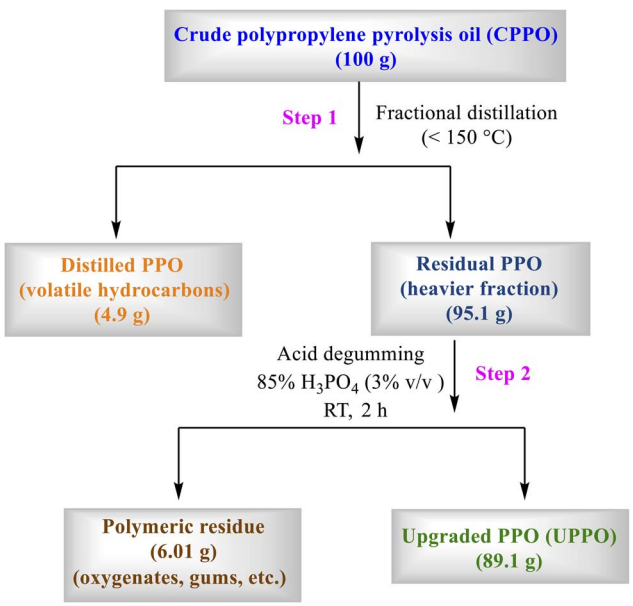

Scheme 1 Schematic representation of the two-step upgrading of CPPO into UPPO, containing process details and mass balance.

polypropylene pyrolysis oil (UPPO) was blended with commercial diesel at different volumetric ratios to assess their combustion properties and emission characteristics in a compression-ignition internal combustion engine.

2.4 Characterization of CPPO and UPPO

The chemical composition of the oil samples was determined as the volume percentages of paraffins, olefins, and aromatics by integrating the peaks at various regions of the ^{1}H-NMR spectrum.[28] Similarly, the isoparaffin index and H/C ratio were estimated from the integral areas of peaks in different chemical shift regions, as shown in Table 1.[29]

The following eqn (1)–(5) have been used to calculate the percentages of various types of protons in the molecular components of the PPO samples.[28,29]

$$\text{Aromatic, vol\%} = \frac{\left[\left(A+\frac{C}{3}\right)0.97\times 100\right]}{[(A+C/3)0.97+(D-2B+E/2+F/3)1.02+3.33B]} \quad (1)$$

$$\text{Parafinns, vol\%} = \frac{[(D-2B+E/2+F/3)1.02\times 100]}{[(A+C/3)0.97+(D-2B+E/2+F/3)1.02+3.33B]} \quad (2)$$

$$\text{Olefins, vol\%} = \frac{3.33B\times 100}{[(A+C/3)0.97+(D-2B+E/2+F/3)1.02+3.33B]} \quad (3)$$

$$H/C = \frac{A+B+C+D+E+F}{\left[\left(A+\frac{C}{3}\right)0.97+\left(D-2B+\frac{E}{2}+\frac{F}{3}\right)1.02+3.33B\right]} \quad (4)$$

(4)

$$\text{Isoparaffin index} = \frac{CH_3}{CH_2} = \frac{F/3}{E/3} \quad (5)$$

2.5 Preparation of fuel blends

UPPO was blended (10–25 vol%) with petrodiesel to study the combustion performance and emission characteristics of the UPPO-diesel blends in a compression-ignition single-cylinder diesel engine. The required volume of UPPO was measured in a calibrated measuring cylinder (100 mL) and introduced into a beaker (2 L). The required quantity of diesel was added using the same measuring cylinder, and the total volume was made up to 1 L. For example, the B10 fuel blend was prepared by mixing 100 mL of UPPO with 900 mL of diesel. A Teflon-coated magnetic stirring rod was introduced in the beaker, and the mixture was stirred at 500 rpm for 1 h. Similarly, 150 mL, 200 mL, and 250 mL UPPO were used to make B15, B20, and B25 UPPO-diesel blends of 1 L volume, respectively. The fuel mixtures were stored in air-tight glass bottles.

Table 1 Types and chemical shift values of the proton signals in the ^{1}H-NMR spectrum of CPPO and UPPO

	Proton type	Chemical shift
A	Aromatic	8.0–6.6
B	Olefin	6.0–4.5
C	Methylene/methane (attached to aromatics/allyl)	3.0–2.0
D	Methine (paraffins)	2.0–1.5
E	Methylene (paraffins)	1.5–1.0
F	Methyl (paraffins)	1.0–0.6

2.6 Engine testing setup and instrumentation

The UPPO-diesel blends were homogenized by magnetic stirring and then filtered through a Whatman filter paper (grade 4) before studying their performance in a single-cylinder compression-ignition engine. The engine setup consisted of a single-cylinder, naturally aspirated, direct-injection, water-cooled diesel engine (make: Kirloskar, model: TV1) coupled to an eddy-current dynamometer as a load. The engine was designed for a power output of 3.5 kW at 1500 rpm. Complete specifications of the single-cylinder diesel engine are shown in the SI file (Table S1, SI).

Single-cylinder diesel engines are widely used as the primary power source for irrigation and decentralized energy production across the Indian subcontinent, particularly in rural and semi-urban areas. Due to their simple design, robustness, and adaptability to a wide range of fuels, these engines are routinely used to test alternative fuels at most research institutions. Fuel consumption was measured using a conventional gravimetric method with a calibrated burette and a stopwatch, enabling accurate determination of the fuel flow rate under varying engine load. A piezoelectric Kistler pressure sensor was mounted on the cylinder to record the in-cylinder combustion characteristics. The pressure signals were digitized and recorded by a high-speed data-acquisition system synchronized with the crank angle encoder. The recorded pressure data were subsequently analyzed using dedicated software for combustion analysis (Engine Soft, Version 9.0). Thermal measurements were obtained using a K-type thermocouple made of Cr–Al alloy interfaced with a temperature sensor. This setup was used to record the temperature of lubrication oil and exhaust gas. The emission of various gases from the exhaust was studied using the INDUS 5 Gas Analyzer (Model: PEA 205N). The fuel consumption was determined volumetrically using a calibrated burette and stopwatch, while the airflow rate was measured manually for each engine load. Initially, the engine was run for 30 minutes at 1500 rpm at a fixed load to reach the steady-state conditions before data recording was initiated. Technical specifications of the exhaust gas analyzer used in the present work are listed in Table S2 of the SI. The photographic images of the engine setup are shown in the SI (Fig. S4–S7).

3. Results and discussion

The following subsections present detailed characterizations of CPPO and UPPO, the preparation of UPPO-diesel blends, their

use as fuels in a diesel engine, and a discussion of their combustion properties and emission characteristics.

3.1 Physicochemical and thermal analyses of CPPO and UPPO

3.1.1 Physical appearance of CPPO and UPPO. Freshly produced CPPO by the thermal pyrolysis of EOL-PP is an orange, free-flowing oil with a diesel-like odor. However, the oil quickly changed color over the next few days, turning from red-brown to nearly black, with a pungent odor and increased viscosity. The deterioration was slowed down to some extent by avoiding exposure to oxygen and sunlight. The rapid deterioration in color and odor of CPPO can be attributed to the presence of unstable compounds, including carbonyl compounds, terminal olefins, and sulfur- and nitrogen-containing heterocycles. The EOL-PP contains partially degraded PP chains due to photooxidation. Moreover, because anaerobic conditions in the pyrolysis reactor are difficult to maintain, additional oxygenates form during the depolymerization reaction. Polycyclic aromatics (*e.g.*, naphthalene), heteroaromatics, and other polyunsaturated compounds absorb light of different wavelengths in the visible region, giving the oil a darker color. Additives in plastic waste, such as stabilizers and plasticizers, also degrade during pyrolysis and end up in CPPO. These unstable compounds undergo secondary reactions (*e.g.*, condensation) during storage, forming coloured products. The sulfur-containing compounds originate from the degradation of various additives and contaminants in EOL-PP, resulting in a pungent smell. The oxidation of carbonyl compounds (*e.g.*, aldehydes) leads to carboxylic acids and is responsible for the acidity of CPPO. Acidic compounds further degrade the oil and can corrode metal parts when used as fuel in engines and furnaces. Upgrading CPPO aims to remove or reduce unstable and undesired components without requiring significant energy or material input. In this first step of upgrading CPPO, fractional distillation under atmospheric pressure removed the volatile compounds (b.p. <150 °C). This fraction, termed DPPO-N (Fig. 2) is responsible for the very low flash point of CPPO, which makes it a poor choice for a diesel substitute. The molecular composition of DPPO-N was studied by GC-MS (Fig. S3, SI). The thermal treatment helps unstable compounds react with each other and partially precipitate. In the second step, the polar (*e.g.*, oxygenates) and oligomerized components were separated from the residual PPO by treating with a strong Brønsted mineral acid, such as H_3PO_4, H_2SO_4, and polyphosphoric acid (PPA). These acids assisted in removing sulfur-containing compounds, oxygenates, and oligomerized compounds. The color of UPPO after the acid degumming process improved significantly, viscosity decreased, and odor improved.

3.1.2 Quantitative analysis of the upgradation of CPPO. The mass balance of each fraction and weight loss during the two-step upgrading of CPPO into UPPO was studied. Starting with 100 g of CPPO, the fraction distillation (Step 1) at atmospheric pressure resulted in the removal of 4.9 g of lighter fractions (boiling point <150 °C), indicating the presence of volatile hydrocarbons as confirmed by the ^{1}H-NMR and GC-MS analyses. The remaining heavier fraction (DPPO) was further upgraded by acid degumming with 4.7 g (3%, v/v) orthophosphoric acid (85%, aq.). The degumming process was performed by magnetically stirring the biphasic mixture at RT for 2 h. Thereafter, the stirring was stopped, and the top layer was carefully decanted to get 89.1 g of UPPO. Approximately 6.01 g of mass reduction was observed during degumming, attributed to the removal of polar impurities, gums, and oligomeric species, which were separated as a viscous black liquid. Overall, the process demonstrates efficient upgrading with minimal (<11 wt%) loss of CPPO, with 5% as a high-value coproduct (*i.e.*, the volatile fraction).

3.1.3 Physicochemical and thermal properties of CPPO and UPPO. The physicochemical properties of CPPO, UPPO, and various UPPO-diesel blends were measured using ASTM standard methods. Kinematic Viscosity was measured using the ASTM D7042-21a method with a Stabinger Viscometer at 40 °C, yielding kinematic viscosity in cSt (centistokes) or $mm^2\ s^{-1}$. Density was measured using the ASTM D4052-22 method at 15 °C. The liquid sample (2 mL) was fed into the U-shaped oscillating tube, and an electronic excitation system adjusted the oscillating frequency based on calibration data to account for changes in the U-tube's mass. The fuel density was displayed in the instrument in g mL^{-1} units. An Optical Automatic Pour Point Apparatus was used to measure the pour points of the fuel blends using the D5950-14 technique. The movement of the cooled liquid was monitored by tilting it at 1 °C or 3 °C intervals. The limiting range was −9 °C to −19 °C. Sulfur content was measured by using the D7220-22 method using

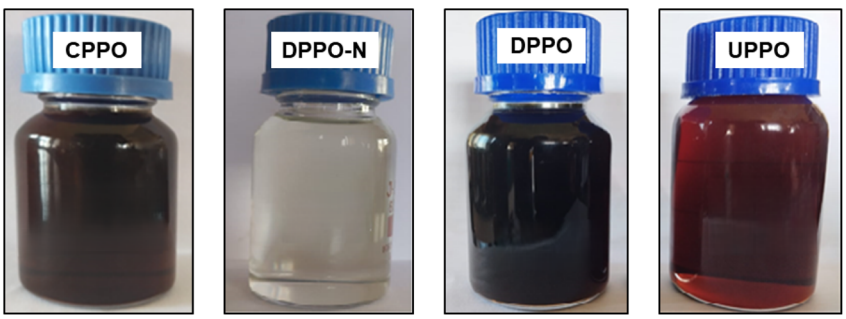

Fig. 2 Photographic images of the PPO samples at various stages of upgrading.

a monochromatic X-ray Fluorescence Analyzer and an X-ray detector with a resolution value of <175 eV at 5.9 Kcps. The regulative value for sulfur content in diesel is 10 ppm. Acid number was determined by volumetric titration using *p*-naphtholbenzein as an endpoint indicator following ASTM D974-22 method. It is measured as the milligrams of KOH required to titrate the acid present in 1 g of the oil sample, and the expected value should be <0.5 mg KOH. Following the standard D93-20, the flash point of the fuel was measured using a Pensky–Martens Closed Cup Apparatus and was expected to be above 35 °C. The calorific value was measured using the D240-19 method, expressed in MJ kg^{-1}. These comparative features are essential for determining the fuel properties and emission characteristics of UPPO as a diesel substitute.

The upgradation of PPO by distillation followed by degumming significantly improved the physicochemical properties of UPPO, with most values conforming to regulatory guidelines and being comparable to those of diesel fuel (Table 2). The calorific value of UPPO improved to 45.99 MJ kg^{-1} from 44.88 MJ kg^{-1} in CPPO, suggesting the elimination of oxygenates during the two-step upgrading process. The second-step degumming process removed oxygenates and acidic compounds (*e.g.*, carboxylic acids) from CPPO, resulting in a significant decrease in the acid value. The acid value of CPPO was 5.82 mg KOH per g, whereas that of UPPO was only 0.54 mg KOH per g. A decrease in the sulfur content in UPPO (compared to CPPO) was also observed, but it was higher than the acceptable value in petrodiesel. Therefore, a desulfurization step may be added to improve the values. In this study, UPPO was blended (*i.e.*, 10–25 vol%) with commercial diesel to minimize any complications. For example, for 20 vol% UPPO blended with diesel (*i.e.*, B20), the sulfur content will be around 12 ppm.

3.2 Compositional and spectral analyses

3.2.1 Analysis of molecular composition by gas chromatography (GC). The molecular composition of CPPO and UPPO was analyzed using GC-MS. The molecules were identified by comparing their similarity indices with those of the compounds in the database. The compounds were segregated by the number of carbon atoms in their molecular structures. The GC analyses showed that CPPO contained a broad range of compounds, ranging from C5 to C40. The volatile fraction (C5–C11) has a significant presence on CPPO, which explains its low flash point (<20 °C, closed cup). A large fraction of C8 compounds was noticeable (Fig. 3). Most of the compounds in CPPO had a carbon number between C8 and C25. After the two-step upgrading, UPPO showed a markedly different molecular profiling. It was found that the volatile fraction (C5–C11) was completely removed from CPPO by fractional distillation in the first step of the upgrading process. The data was supported by the molecular composition of DPPO-N (Table S3, SI). Most of the compounds in UPPO contain C13–C31 compounds, while the maximum fraction contains C17 (diesel range). Therefore, the flash point of UPPO significantly improved to that of diesel.

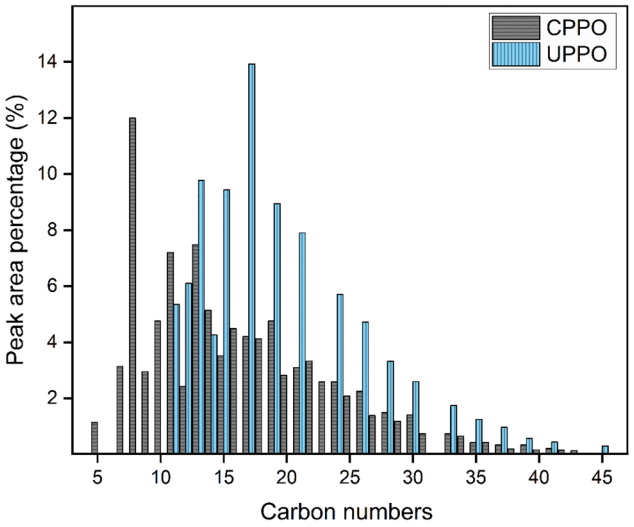

Fig. 3 Peak area percentage of carbon numbers in the molecules in UPPO and CPPO.

3.2.2 Analyses of CPPO and UPPO by FTIR spectroscopy. Fourier transform infrared spectroscopy (FTIR) is a spectroscopic technique primarily used to identify the functional groups of organic molecules. FTIR helps to identify aliphatics, aromatics, carbonyl compounds, and other oxygenates in a fuel mixture. As evident from the overlayed FTIR spectra of CPPO and UPPO in Fig. 4, there was no stark difference between the spectra. The observation may be due to aliphatic hydrocarbons dominating both CPPO and UPPO. The peaks from minor compounds containing specific functional groups remain subdued in the overwhelmingly intense peaks of the aliphatic hydrocarbons. There are four peaks around 3000 cm^{-1}, two of which originate from the asymmetric and symmetric C–H stretching frequency of the methylene ($-CH_2-$) groups. The other two peaks originate from the asymmetric and

Table 2 Comparison of some physicochemical and thermal properties of diesel, CPPO, and UPPO

Physicochemical properties	ASTM methods	Unit	Diesel	CPPO	UPPO
Density (15 °C)	D4052-22	g cm^{-3}	0.831	0.799	0.812
Kinematic viscosity (40 °C)	D7042-21a	cSt	2.781	2.126	3.385
Flash point	D93-20	°C	47	<20	47.5
Pour point	D5950-14	°C	−6	−24	−9
Acid value	D974-22	mg KOH per g	0.06	5.82	0.54
Sulfur content	D7220-22	ppm	6	46.5	38
Calorific value	D240-19	MJ kg^{-1}	45.50	44.88	45.99

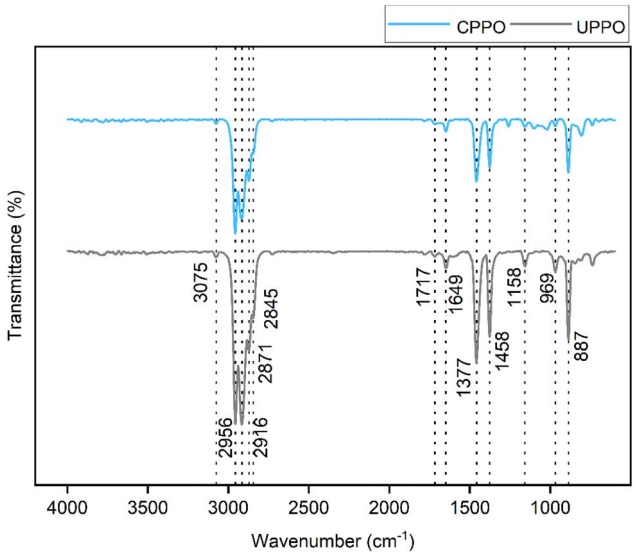

Fig. 4 The overlayed CPPO (blue) and UPPO (grey) FTIR spectra.

antisymmetric C–H stretching frequency of the methyl ($-CH_3$) groups. The intense peak at 2956 cm^{-1} signifies the C–H stretching frequency of the methyl groups, whereas the peak at 2916 cm^{-1} is due to the asymmetric C–H stretching frequency of the methylene groups. The 1458 cm^{-1} peak is due to the symmetric C–H stretching frequency of the methyl groups, whereas the 1377 cm^{-1} peak appears owing to the symmetric C–H stretching frequency of the methylene groups. The 3076 cm^{-1} peak is due to the C(sp^2)-H stretching from olefins and aromatic compounds. The peak at 1717 cm^{-1} is due to carbonyl groups (*e.g.*, ketones and carboxylic acids). The peak at 1649 cm^{-1} may correspond to the C=C stretching frequency of olefins. The peak at 1458 cm^{-1} is due to the bending (scissoring) vibration of methyl and methylene groups. The peak at 1377 cm^{-1} is due to the bending vibration (umbrella mode) of the methyl groups. Peaks in the fingerprint region 968 cm^{-1}, 887 cm^{-1}, 845 cm^{-1}, 811 cm^{-1}, and 738 cm^{-1} are also of C–H bending vibration but of the aromatic ring. The C–O stretching appeared around 1100 cm^{-1} in CPPO, suggesting the presence of oxygenates, which reduced significantly in UPPO.

3.2.3 Analyses by ^{1}H-NMR spectroscopy. ^{1}H-NMR spectroscopy provides details on the chemical composition of CPPO and UPPO, which is crucial for determining the efficiency of the upgrading process. Fig. 5 shows the ^{1}H-NMR spectra of CPPO and UPPO in $CDCl_3$, collected on a 300 MHz NMR spectrometer. The ^{1}H-NMR spectrum of CPPO shows multiple peaks of saturated aliphatic protons between 0.71 and 1.0 ppm. Peaks between 1.0 and 1.5 ppm appear due to methylene protons. These peaks with a significant integral area suggest the presence of long saturated hydrocarbon chains in CPPO. Multiple peaks between 4.55 and 4.62 ppm are due to olefinic protons and oxygenates. Weak peaks around 7.15 ppm are due to aromatic protons. The ^{1}H-NMR spectrum of UPPO showed

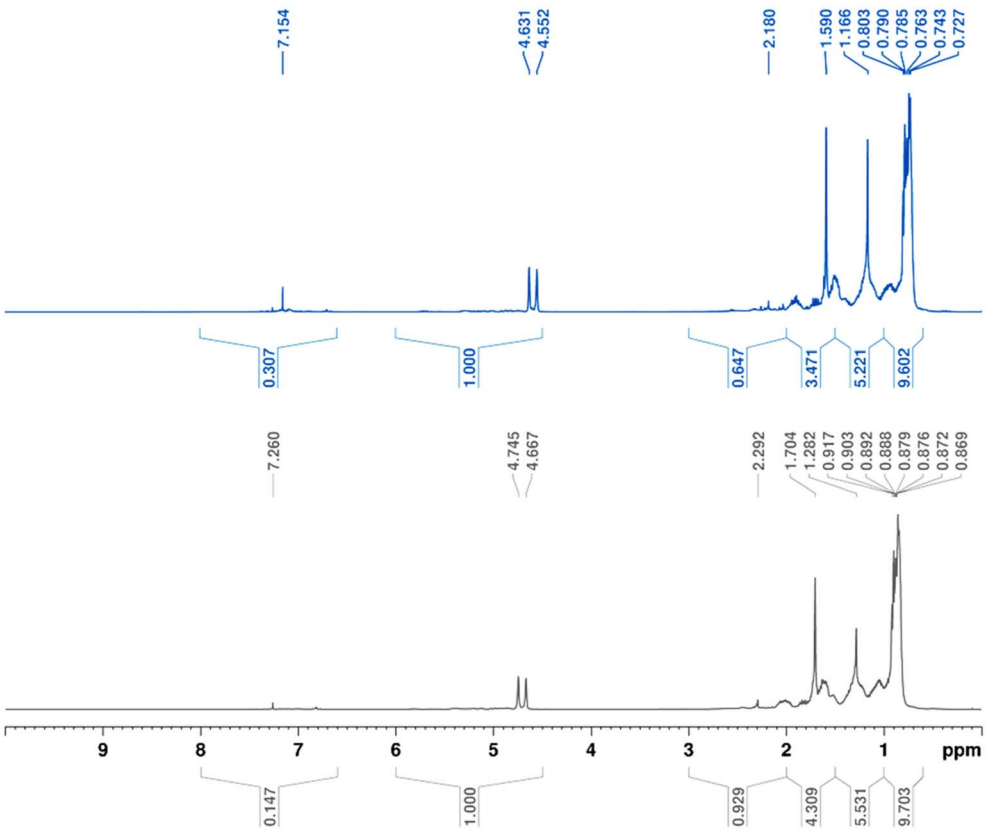

Fig. 5 The ^{1}H-NMR spectrum of CPPO (blue) and UPPO (grey).

Table 3 The ^{1}H NMR spectral regions and corresponding integral area in CPPO and UPPO

	Proton type	Chemical shift	Integral area of CPPO	Integral area of UPPO
A	Ring aromatic	8.0–6.6	0.31	0.15
B	Olefin	6.0–4.5	1	1
C	α-Methyl	3.0–2.0	0.65	0.93
D	Methine (paraffins)	2.0–1.5	3.45	4.31
E	Methylene (paraffins)	1.5–1.0	5.22	5.53
F	Methyl (paraffins)	1.0–0.6	9.60	9.70
	Aromatics, vol%		0.8	0.79
	Paraffins, vol%		65	69.2
	Olefins, vol%		29	26.7
	H/*C*		1.8	1.73
	Isoparaffin index		1.23	1.24

a more intense multiplet between 0.90 ppm and 1.61 ppm, suggesting a greater amount of saturated aliphatic hydrocarbons than in CPPO. The peak at 2.29 indicates the presence of methylene (CH_2) protons. A doublet between 4.66 and 4.74 ppm represents the presence of olefinic protons or methylene/methine groups attached to electronegative atoms (*e.g.*, O), but present in a smaller percentage than CPPO. Two small peaks between 6.5 and 7.5 ppm suggest the presence of aromatic protons. Table 3 lists the types of proton signals in the ^{1}H-NMR spectrum, along with the volume percentages of aromatics, paraffins, and olefins, the isoparaffin index, and the H/C ratios of CPPO and UPPO. There was a slight increase in the vol% of paraffin from 65% in CPPO to 69.2% in UPPO. On the contrary, the vol% of olefins decreased from 29% in CPPO to 26.7% in UPPO. This change in composition also explains the improved storage and thermal stability of UPPO compared to CPPO. There was no noticeable change in the volume percentage of aromatic compounds after upgradation. Such changes are expected to improve the combustion properties of UPPO in a diesel engine. Some major molecular components in UPPO, after the two-step upgrading, have been listed (Table S4, SI).

3.2.4 Quantitative analysis of CPPO and UPPO by NMR. The ^{1}H-NMR spectroscopic technique can be used as a reliable quantitative technique to determine the molecular composition in a mixture of NMR-responsive small organic molecules. Dimethyl terephthalate (DMT) was used as the internal standard owing to its non-volatile nature, solubility in hydrocarbons, and well-resolved, simple ^{1}H-NMR spectrum (a singlet for six methyl protons and a singlet for four aromatic protons). A known quantity (20 mg) of DMT and PPO (CPPO and UPPO) was dissolved in $CDCl_3$, and ^{1}H-NMR spectra were recorded. The integration of characteristic proton signals corresponding to the methyl protons of DMT in quantitative NMR of CPPO and UPPO enabled the determination of absolute changes in the composition of aromatics, paraffins, olefins, H/C, and the isoparaffin index during the upgradation process. It was observed that the aromatics vol% decreases from 5.26 to 3.77 vol% for UPPO. The vol% of paraffins and olefins in CPPO and UPPO remains nearly the same, whereas a slight increase in H/C and the isoparaffin index for UPPO was observed compared to CPPO. The composition of CPPO and UPPO is mentioned in Table S5 of the SI. The ^{1}H-NMR spectrum of CPPO and UPPO using DMT as an internal standard is shown in Fig. S8 & S9 of the SI.

3.2.5 Analyses of the degummed fraction by NMR. The polymeric residue obtained after the second step of upgrading (*i.e.*, acid degumming process) was thoroughly washed and neutralized. The neutralized degummed fraction was then characterized by ^{1}H-NMR spectroscopy to analyze the chemical composition of the degummed residue. The degummed fraction exhibits a higher aromatic content (20 vol%) compared to both CPPO and UPPO. This apparent increase can be attributed to the removal of polar impurities, gums, unstable polymers and oligomers, and heteroatom-containing compounds. The ^{1}H-NMR spectrum of the gummy fraction is shown in Fig. S10 of the SI. The gummy fraction consisted of approximately 62 vol% of paraffins, 17.2 vol% of olefins, and 20 vol% of aromatics.

3.3 Fuel properties analysis of various blends

Density of the UPPO-diesel fuel blends (B10, B15, and B20) was comparable to unblended diesel. More specifically, the density of unblended diesel and the B25 blend were 0.831 g cm^{-3} and 0.829 g cm^{-3}, respectively, at 15 °C. Kinematic viscosity (at 40 °C) of the UPPO-diesel blends did not show any specific trend and were within acceptable limits. The pour point of the unblended diesel was −6 °C, whereas the blends showed a marginal increase to −3 °C. The pour point of the fuel is a crucial property for assessing cold–flow properties, and all the UPPO-diesel blends performed satisfactorily. The flash point, acid value, and calorific value of the fuel mixtures studied in

Table 4 Selected physicochemical characteristics of the fuel blends

Properties	Unit	Diesel	B10	B15	B20	B25
Density at 15 °C	g cc^{-1}	0.831	0.832	0.827	0.829	0.826
Kinematic viscosity (40 °C)	cSt	2.781	2.782	2.757	2.802	2.825
Acid value	mg KOH per g	0.06	0.14	0.15	0.18	0.16
Flash point	°C	47	45	44.5	44	44.5
Pour point	°C	−6	−3	−3	−3	−6
Sulfur content	ppm	6	10	11.5	14.5	13.5
Calorific value	MJ kg^{-1}	45.5	45.8	45.7	45.9	46.2

this work were within the acceptable limits of diesel fuel. Table 4 lists some major physicochemical properties and their experimentally determined values for unblended diesel and UPPO-diesel blends.

3.4 Utilization of UPPO-diesel fuel blends in the diesel engine

3.4.1 Combustion characteristics and engine performance. The favorable physicochemical properties of diesel and UPPO-diesel blends promise efficient combustion in the compression-ignition internal combustion engine. One of the most widely used parameters for determining a fuel's combustion efficiency in a diesel engine is the brake thermal efficiency (BTE). BTE is defined as the ratio of the mechanical power output of an engine (brake power) to the rate of energy input from the fuel. It measures how effectively an engine converts the chemical energy stored in the fuel is transformed into useful mechanical work. BTE increases with engine load, and the same trend was observed in all the fuels used in this study. BTE in the UPPO-diesel blends (B10, B15, B20, and B25) was observably higher than unblended diesel. Therefore, the UPPO-diesel blends enabled more efficient conversion of chemical energy into useful work, suggesting better fuel economy and cleaner combustion. A higher BTE indicates that heat escaping into the exhaust is reduced. Fig. 6 shows the variation of BTE with engine loads (0–100%) using various fuel blends.

The brake-specific energy consumption (BSEC) is an important performance parameter that evaluates the energy efficiency of internal combustion engines, and it is used to determine the efficiency of converting heat energy into mechanical power. BSEC expresses the total energy input required to produce one kilowatt-hour of brake power. A lower BSEC indicates that the engine converts the fuel's chemical energy into useful mechanical energy more efficiently. Fig. 7 shows that the BSEC decreases with increasing load, indicating that the various blends perform more efficiently at higher loads than at lower

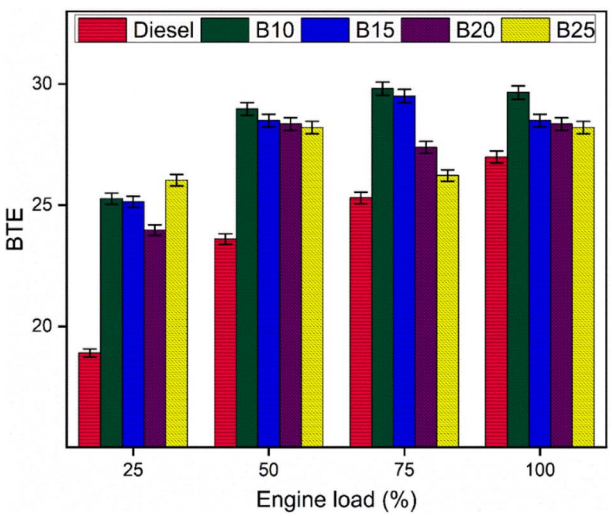

Fig. 6 Variation of brake thermal efficiency (BTE) with engine load.

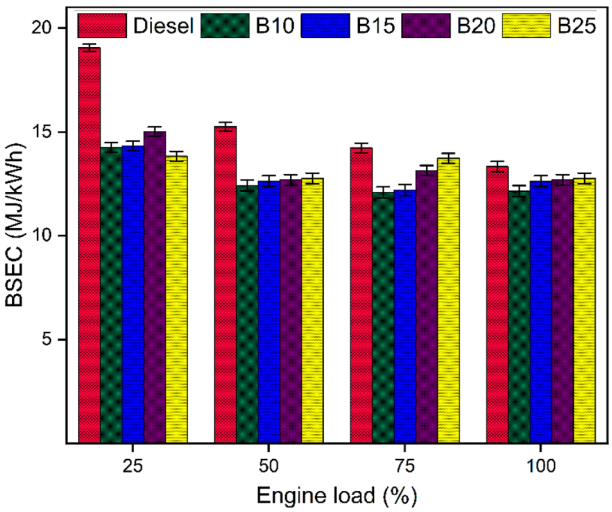

Fig. 7 Variation of brake specific energy consumption (BSEC) with engine load.

ones. It was observed that the BSEC decreases from pure diesel to various fuel blends and remains almost constant with increasing blend percentage. The higher volatility of UPPO improves fuel atomization and homogenizes the air–fuel mixture, leading to more efficient combustion and reduced energy waste, thereby increasing the BTE. As a result, the engine requires less fuel energy input per unit of brake power output for the UPPO-diesel blends than for unblended diesel fuel.

Uncertainty analysis was performed to assess the accuracy of the instrumental data. The uncertainty in BTE was calculated using the root-sum-square approach. The uncertainty analysis is included in the SI (Page S2, SI) based on the published literature.[30,31]

3.4.2 Combustion analysis. Combustion efficiency in the compression-ignition internal combustion engine can be assessed using in-cylinder pressure (CP-max) and the mean gas temperature (MGT). CP-max is the peak pressure reached in the cylinder during combustion of the compressed fuel-air mixture. For a fixed engine load, the CP-max data from 100 engine cycles were averaged to record the value for the fuel under analysis (Fig. 8). The fuel blends may show different ignition characteristics depending on the volatility of the molecular components. If a blend produces advanced (early) combustion phasing, the CP-max may be raised. On the contrary, when a fuel blend burns slowly (due to slow evaporation or delayed ignition), it results in a lower CP-max. The CP-max of pure diesel and UPPO-diesel blends increased at higher engine load. As engine load increases, more fuel is required to meet the power demand. The large amount of heat released and high combustion temperature increase the CP-max. The B10, B15, and B20 fuel blends showed a noticeable reduction in CP-max at all engine loads compared to unblended diesel. However, the B25 blend showed a larger CP-max than the other blends, but still lower than diesel.

MGT is a critical parameter that provides insight into heat release and use during the engine's compression, combustion,

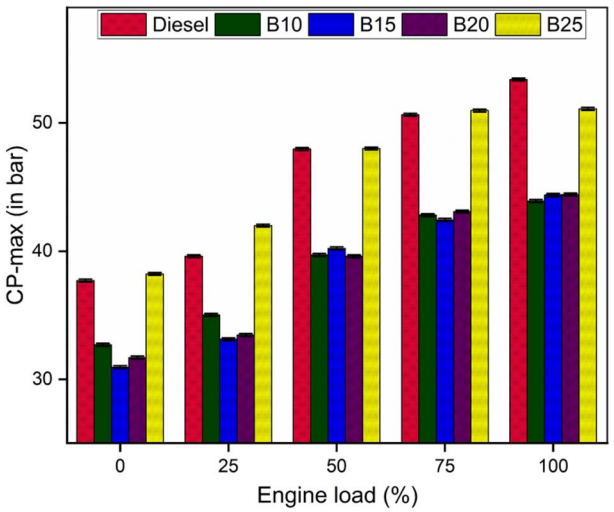

Fig. 8 The maximum in-cylinder pressure at various engine loads.

and expansion strokes. MGT refers to the average temperature of the gases inside the combustion chamber over a complete engine cycle. It signifies the thermal state of combustion characteristics, heat transfer, and overall engine performance, providing insights about the heat release inside the cylinder during each engine cycle. The average temperature of 100 MGT cycles was determined for each engine load. A higher MGT generally indicates more efficient combustion and greater heat release, thereby improving the fuel's thermal efficiency. As load increases, MGT generally rises due to increased fuel consumption. More fuel is injected at higher loads, leading to a higher heat release rate and elevating the MGT. This trend indicates improved combustion with increasing engine load. The variation of MGT across diesel and various UPPO-diesel fuel blends is shown in Fig. 9.

At lower engine loads (0–50%), the MGT of B10–B20 fuel blends were comparable with diesel, whereas the B25 fuel blend had noticeably higher values. At higher engine loads (75–100%), all the fuel blends had higher MGT than diesel, especially B25. The higher aromatic content in the UPPO may be responsible for this behavior.

3.4.3 Emission characteristics of UPPO-diesel fuel blends. The emission characteristics of UPPO-diesel blends were studied using the INDUS 5 Gas Analyzer (model: PEA 205N). The emission of nitrogen oxides (NO_x) heavily depends on the in-cylinder temperature during the combustion of fuel. Higher compression of the fuel-air mixture raises combustion temperature, increasing NO_x emissions. In this study, the NO_x emission from unblended diesel increased from 8 ppm at 0% engine load to 285 ppm at 100% engine load (Fig. 10). The NO_x increased from 4 ppm at 0% engine load to 277 ppm at 100% engine load for the B10 fuel blend. The NO_x emission decreased from B10 to B25 due to reduced CP-max, which implies a reduction of NO_x emission at lower combustion temperature. NO_x emissions increased with engine load for unblended diesel and UPPO-diesel blends (B10–B25). The quantity of fuel injected per combustion cycle increases at higher engine loads to fulfill the increased power demand. The combustion of a larger volume of fuel releases more heat. Excess heat significantly increases in-cylinder pressure and MGT, leading to additional NO_x formation. The NO_x emissions of diesel and UPPO-diesel blends remained comparable across all engine loads.

Carbon monoxide (CO) forms from the incomplete combustion of carbon-based fuels in the compression-ignition internal combustion engine. In this study, CO emissions from UPPO-diesel blends were measured at varying engine loads. At 100% engine load, CO emissions decreased for UPPO-diesel blends compared to unblended diesel. The percentage CO emissions of diesel and UPPO-diesel blends at various engine loads are depicted in Fig. 11. With increasing engine load, CO emissions increased slowly across all fuel samples. The combustion process became more vigorous as the engine load reached 100%. The available time for the further oxidation of CO to CO_2 was reduced, leading to a significant increase in CO

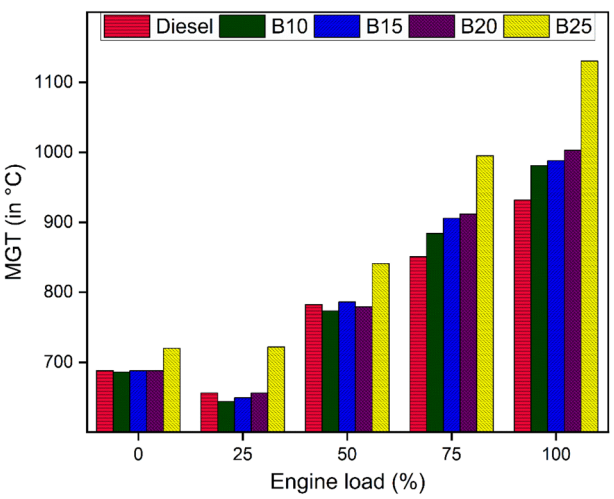

Fig. 9 Variation of the mean gas temperature (MGT) with engine load.

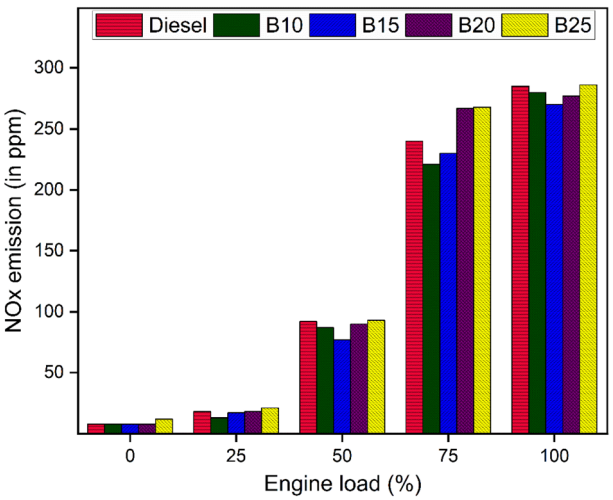

Fig. 10 Emission of NO_x by diesel and UPPO-diesel fuel blends at various engine loads.

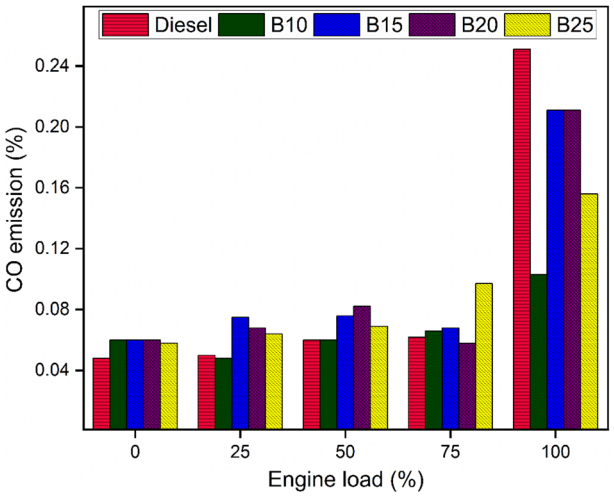

Fig. 11 Emission of CO (%) by diesel and diesel-UPPO fuel blends at various engine loads.

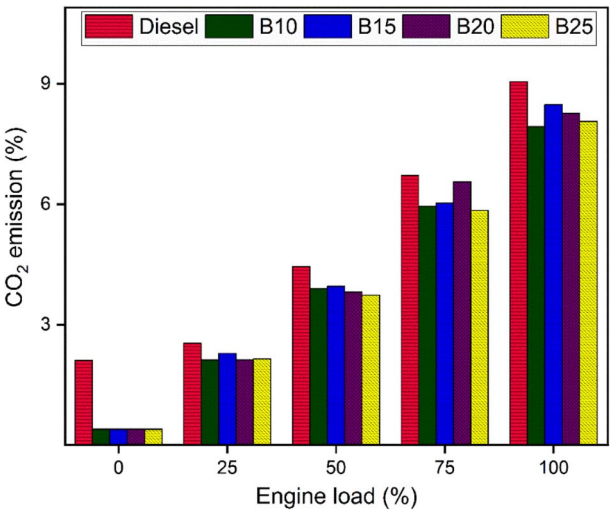

Fig. 12 Emission of CO_2 by diesel and UPPO-diesel blends at various engine loads.

emissions. The UPPO-diesel blends also showed a similar pattern, and CO emissions were comparable to those of diesel, with some variations.

Carbon dioxide emissions indicate the availability of sufficient oxygen in the combustion chamber for complete combustion of the fuels under study. Density, viscosity, oxygenates, molecular composition of the fuels, and the air-fuel ratio influence carbon dioxide emissions. It was noted that diesel had higher CO_2 emissions, whereas CO_2 emissions decreased slightly with increasing UPPO percentage in the UPPO-diesel blends. Since the molecular composition of UPPO was similar to diesel, the impact on CO_2 emissions was less pronounced. Higher engine loads increase CP-max and MGT, thereby enhancing oxidation reactions and elevating CO_2 emissions (Fig. 12).

The emission of unburnt hydrocarbons (UHC) results from the insufficient or incomplete combustion inside the cylinder in

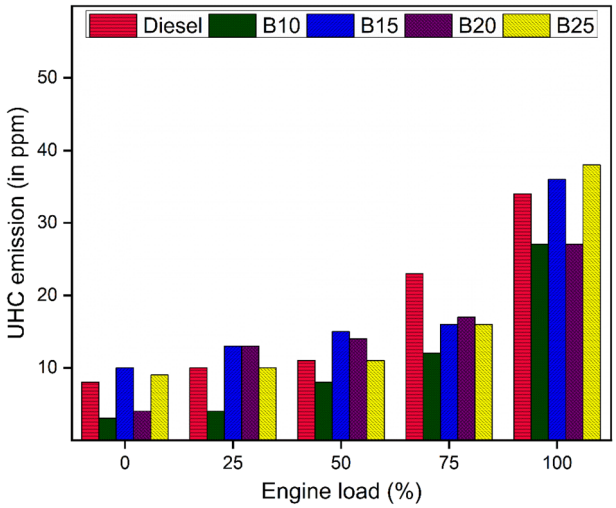

Fig. 13 UHC emission of diesel and diesel-UPPO fuel blends at varying engine loads.

internal combustion engines. Despite some variations, UHC was lowest in the B10 blend and increased as the engine load increased from 0% to 100%. A decrease in UHC is typically observed with increasing engine load, due to improved combustion efficiency at higher in-cylinder temperatures. However, as engine load increases, the required fuel-to-air ratio increases to maintain a safe operating temperature and avoid overheating the cylinder. The published literature reported both increasing and decreasing trends for UHC with increasing engine load. At higher engine loads (*i.e.*, 75% & 100%), UHC decreased noticeably for the UPPO-diesel blends compared to unblended diesel. The presence of oxygenated compounds in UPPO facilitates the complete combustion of the fuel mixture and reduces UHC emissions. The UHC of diesel and UPPO-diesel blends under varying engine loads is shown in Fig. 13.

4. Conclusion

This study demonstrates an effective method for upgrading CPPO to UPPO by selectively removing volatiles and unstable components. The straightforward, scalable upgrade significantly improved the physicochemical and thermal properties, as well as the storage stability, of UPPO, making it a suitable diesel substitute. The UPPO-diesel blends (10–25 vol% of UPPO) showed promising engine performance. For example, the BTE improved in the UPPO-diesel blends across all engine loads compared to unblended diesel, resulting in a decrease in BSEC and indicating improved energy utilization. The maximum cylinder pressure dropped in the UPPO-diesel blends, leading to smoother engine functioning. Compared to unblended diesel, the UPPO-diesel blends resulted in reduced emissions of NO_x, CO, and UHC. This result can be explained by the presence of various oxygenates in UPPO, which reduces the total oxygen requirement for combusting the fuel mixtures and lowers the temperature produced during ignition. The mean gas temperature was comparable in UPPO-diesel blends to that in diesel

alone. Therefore, UHC-diesel blends can be used as cleaner fuels in diesel engines while maintaining engine performance.

Author contributions

Abhishek Kumar Yadav and Suparna Maity performed the experiments and analyzed the data. Sandeep Kumar Yadav helped collect data on the physicochemical characteristics of the fuel blends. Kumar G N and Vasudeva Madav assisted in engine performance, emission analysis, and edited the manuscript. Saikat Dutta conceptualized the work, supervised, and wrote the original manuscript.

Conflicts of interest

The author declares no competing interests.

Data availability

Additional supporting experimental data, photographs of the experimental setup, and the appearance of the fuel blends are available in the supplementary information (SI). Supplementary information is available. See DOI: https://doi.org/10.1039/d5ra09026a.

Acknowledgements

SD thanks the Science and Engineering Research Board (SERB), India, for research funding under the Core Research Grant (CRG) scheme (file no. CRG/2022/009346). The authors thank the central library of NITK, Surathkal, for providing access to academic journals and databases. The authors thank the Internal Combustion Laboratory at the Department of Mechanical Engineering, NITK, Surathkal.

References

1 M. T. Hossain, M. A. Shahid, N. Mahmud, A. Habib, M. M. Rana, S. A. Khan and M. D. Hossain, *Discover Nano*, 2024, **19**, 2.
2 V. Mannheim and Z. Simenfalvi, *Polymers*, 2020, **12**, 1901.
3 J.-P. Lange, *ACS Sustainable Chem. Eng.*, 2021, **9**, 15722–15738.
4 J. Uebe, Z. Kryzevicius, R. Majauskiene, M. Dulevicius, L. Kosychova and A. Zukauskaite, *Waste Manage. Res.*, 2022, **40**, 1220–1230.
5 C. Park and J. Lee, *Int. J. Energy Res.*, 2021, **45**, 13088–13097.
6 A. I. Eldahshory, K. Emara, M. S. Abd-Elhady and M. A. Ismail, *Sci. Rep.*, 2023, **13**, 11766.
7 P. Rex, M. K. Rahiman, P. Barmavatu, S. B. Aryasomayajula Venkata Satya Lakshmi and N. Meenakshisundaram, *Environ. Qual. Manag.*, 2024, **33**, 501–511.
8 R. Geyer, J. R. Jambeck and K. L. Law, *Sci. Adv.*, 2017, **3**, e1700782.
9 L. Zou, R. Xu, H. Wang, Z. Wang, Y. Sun and M. Li, *Natl. Sci. Rev.*, 2023, **10**, nwad207.
10 M. M. Harussani, S. M. Sapuan, U. Rashid, A. Khalina and R. A. Ilyas, *Sci. Total Environ.*, 2022, **803**, 149911.
11 M. J. B. Kabeyi and O. A. Olanrewaju, *J. Energy*, 2023, **2023**, 1–25.
12 M. Laghezza, S. Fiore and F. Berruti, *J. Anal. Appl. Pyrolysis*, 2024, **179**, 106479.
13 Y. Cui, Y. Zhang, L. Cui, Y. Liu, B. Li and W. Liu, *J. Cleaner Prod.*, 2023, **411**, 137303.
14 A. Mohan, S. Dutta, S. Balusamy and V. Madav, *RSC Adv.*, 2021, **11**, 9807–9826.
15 P. Gijsman and R. Fiorio, *Polym. Degrad. Stab.*, 2023, **208**, 110260.
16 M. S. Klippel and M. F. Martins, *Polym. Degrad. Stab.*, 2022, **204**, 110090.
17 M. I. Jahirul, F. Faisal, M. G. Rasul, D. Schaller, M. M. K. Khan and R. B. Dexter, *Energy Rep.*, 2022, **8**, 730–735.
18 P. Palmay, C. Medina, C. Donoso, D. Barzallo and J. C. Bruno, *Clean Technol. Environ. Policy*, 2023, **25**, 1539–1549.
19 H. Wang, M. van Akker, J. G. M. Winkelman, A. Heeres and H. J. Heeres, *Energy Fuels*, 2025, **39**, 3564–3574.
20 L. Briones, A. Cordero, M. Alonso-Doncel, D. P. Serrano and J. M. Escola, *Appl. Catal., B*, 2024, **341**, 123359.
21 M. Sogancioglu Kalem, *Sep. Purif. Technol.*, 2022, **300**, 121859.
22 W. Zeb, T. De Somer, M. Roosen, P. Knockaert, M. S. Abbas-Abadi, U. Kresovic, J. Hogie, K. M. Van Geem and S. De Meester, *Fuel*, 2025, **379**, 133055.
23 T. G. Kailas, A. A R, S. Dutta and V. Madav, *Energy Convers. Manage.:X*, 2025, **25**, 100824.
24 A. Mohan, S. Dutta and V. Madav, *Fuel*, 2019, **250**, 339–351.
25 G. Wei, Z. Chen, X. Tai, Z. Sun and X. Wang, *Trans. Tianjin Univ.*, 2025, **31**, 390–402.
26 C. Allegretti, A. Bono, P. D'Arrigo, F. G. Gatti, S. Marzorati, L. A. M. Rossato, S. Serra, A. Strini and D. Tessaro, *ChemistrySelect*, 2021, **6**, 9157–9163.
27 A. Demydova and T. Berezka, *Innovative Biosyst. Bioeng.*, 2021, **5**, 105–116.
28 M. E. Myers, J. Stollsteimer and A. M. Wims, *Anal. Chem.*, 1975, **47**, 2010–2015.
29 P. Das and P. Tiwari, *Resour., Conserv. Recycl.*, 2018, **128**, 69–77.
30 A. K. Yadav, S. K. Yadav, G. N. Kumar, V. Madav and S. Dutta, *RSC Adv.*, 2025, **15**, 27933–27940.
31 J. Manu, T. G. Kailas and V. Madav, *J. Cleaner Prod.*, 2023, **419**, 137991.